A field investigation on debris flows in the incised Tongde sedimentary basin on the northeastern edge of the Tibetan Plateau

Liqun Lyu[1], Mengzhen Xu[2], Zhaoyin Wang[2], Yifei Cui[3], and Koen Blanckaert[4]

[1]Beijing Forestry University
[2]Tsinghua University
[3]State Key Laboratory of Hydroscience and Engineering, Tsinghua University
[4]Vienna University of Technology

November 23, 2022

Abstract

An investigation on 152 gullies along the Daheba River in the Tongde sedimentary basin was performed. Debris flows develop in gullies with an excess topography Z_E, which represents the sediment availability, above a critical threshold value. Debris-flows in the Daheba watershed are supply-unlimited, i.e sediment is abundantly available from the steep erodible gully banks. Debris flows consist of a head and a body. The body propagates faster than the head and constantly supplies it with sediment. The body and head propagate in an intermittent way through the transient storage of sediment on the riverbed and its subsequent remobilization. Although the main sediment supply is provided by bank collapse, debris-flow events also incise the gully bed. The growth and incision of debris-flow gullies in supply-unlimited watersheds is mainly controlled by the frequency of occurrence of debris flows, which is closely related to Z_E. With growth of the gully drainage area, Z_E and the debris-flow frequency initially increase, until they reach maximum values in gullies with a drainage area of intermediate size, which are assumed to be the morphologically most active gullies. With further growth of the gully drainage area, Z_E and the debris-flow frequency decrease, which opposes the development of debris flows and leads to a more stable gully morphology. The observations indicate and explain the upstream migrating incision of the Daheba watershed. The lack of available sediment in the mountain reach is supposed to limit the further upstream migration of the reach of most active debris flows.

Hosted file

`tables.docx` available at https://authorea.com/users/541421/articles/600614-a-field-investigation-on-debris-flows-in-the-incised-tongde-sedimentary-basin-on-the-northeastern-edge-of-the-tibetan-plateau

A field investigation on debris flows in the incised Tongde sedimentary basin on the northeastern edge of the Tibetan Plateau

Liqun Lyu[1*], Mengzhen Xu[2*], Zhaoyin Wang[2], Yifei Cui[2], Koen Blanckaert[2,3]

[1] School of Soil and Water Conservation, Beijing Forestry University, Beijing 100083，PR China

[2] State Key Laboratory of Hydroscience and Engineering, Tsinghua University, Beijing100084，PR China

[3] Institute of Hydraulic Engineering and Water Resources Management, Technische Universität Wien, 1040 Vienna, Austria

*Corresponding author : Liqun Lyu (lvliqunqinghua@126.com); Mengzhen Xu (mzxu@mail.tsinghua.edu.cn)

Key Points:

- The sediment availability, parameterized by the excess topography Z_E is the dominant control parameter in debris-flow gullies with unlimited sediment supply.
- Although debris flow events incise the bed, the sediment supply during debris-flow events in supply-unlimited gullies mainly comes from bank collapse.
- Debris flow gullies of intermediate size have the highest Z_E and debris-flow occurrence frequency, and are therefore supposed to be morphologically the most active.

Abstract:

An investigation on 152 gullies along the Daheba River in the Tongde sedimentary basin was performed. Debris flows develop in gullies with an excess topography Z_E, which represents the sediment availability, above a critical threshold value. Debris-flows in the Daheba watershed are supply-unlimited, i.e sediment is abundantly available from the steep erodible gully banks. Debris flows consist of a head and a body. The body propagates faster than the head and constantly supplies it with sediment. The body and head propagate in an intermittent way through the transient storage of sediment on the riverbed and its subsequent remobilization. Although the main sediment supply is provided by bank collapse, debris-flow events also incise the gully bed. The growth and incision of debris-flow gullies in supply-unlimited watersheds is mainly controlled by the frequency of occurrence of debris flows, which is closely related to Z_E. With growth of the gully drainage area, Z_E and the debris-flow frequency initially increase, until they reach maximum values in gullies with a drainage area of intermediate size, which are assumed to be the morphologically most active gullies. With further growth of the gully drainage area, Z_E and the debris-flow frequency decrease, which opposes the development of debris flows and leads to a more stable gully morphology. The observations indicate and explain the upstream migrating incision of the Daheba watershed. The lack of available sediment in the mountain reach is supposed to limit the further upstream migration of the reach of most active debris flows.

Key words: Debris flow; Landscape evolution; Sedimentary basin; Field investigation; sediment availability

1. Introduction

1.1: general context

Debris flows occur when masses of poorly sorted sediment (sand, mud, boulders, cobbles), agitated and saturated with water, surge down slopes in deep gullies in response to gravitational acceleration (Iverson 1997, Hungr et al. 2001). A gully is defined as a long narrow valley with steep side slopes, which is originally worn in the earth by running water and which drains water and sediment after rain. From upstream to downstream, a gully consists of a steep gully head, a steep and narrow middle reach, and a depositional fan (Fig. 1).

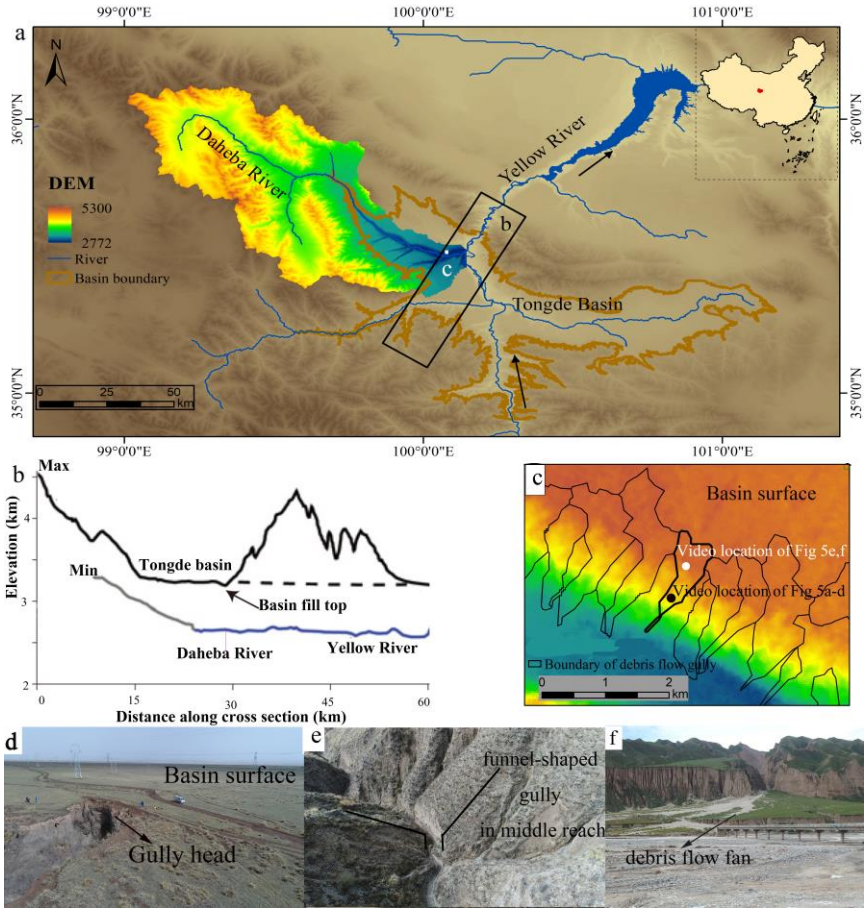

Figure 1. (a) Tongde sedimentary basin, Yellow River and its tributary Daheba River on the northeastern Tibetan plateau, and DEM of the watershed of the Daheba River; (b) Maximum and minimum elevation along the 20-km-wide swath indicated in Fig. 1a. Blue segments in the minimum elevation profile coincide with the Yellow River (modified from Craddock et al, 2010). (c) DEM-based identification of gully watersheds; the thick line indicates the watershed of the gully at km 11.4; (d) Surface of Tongde basin and head of the gully at km 11.4; (e) Funnel-shaped cross-section in the middle reach of the gully at km 11.4; (f) Fan of the debris-flow gully at km 11.4 characterized by high gradient and coarse mixture of gravel and sand.

Debris flows in mountain regions can travel long distances under high-rainfall conditions and result in loss of human lives, damage to buildings, farm fields or transport infrastructure (roads, railways, etc), and vegetation denudation (Papathoma-Köhle et al. 2012; Winter et al. 2013; Godfrey et al. 2015; Ciurean et al. 2017).

The higher debris surge at the front of the debris flows is called the debris-flow head (Kattel et al., 2016). Boulders and cobbles play an important role in its formation, and it is characterized by low water content (Suwa, 1988; Iverson, 1997; Takahashi, 2009; Johnson et al. 2012; Luna et al., 2012). Wang et al. (2005) even observed debris flows with only dry stones moving in the head. Because of the boulders and cobbles, the debris-flow head can exert high impulsive loads on objects it encounters. The debris-flow head is followed by the debris-flow body (Kattel et al., 2016), which is characterized by smaller sediment sizes and high water content with water flowing at the surface of the body (Luna et al., 2012).

Debris flows entrain sediment during their run-out. This sediment can be supplied by erosion of the gully bed and banks (Imaizumi et al., 2006; Theule et al., 2012). Erosion of the gully bed includes breaching of temporary dams, and erosion of the banks includes bank collapses or landslides (Zhou et al., 2019). The motion of debris flows is obviously influenced by the distribution of the sediment in a gully (Berger et al., 2011). Pudasaini (2012) presented a comprehensive process-based model of debris flows.

The initiation and frequency of occurrence of debris flows essentially depend on two factors. First, they depend on the volume of sediments that can be mobilized in the catchment and its renewal rate. These in turn depend on the geological conditions (e.g., lithology, tectonic faults) (Griffiths et al. 1996; Jomelli et al. 2007; Lorente et al. 2002; McCoy et al. 2012), morphometry of the gully area (Kovanen

and Slaymaker 2008; Bertrand et al. 2013) and land cover (Reichenbach et al. 2014). Second, they depend on the rainfall characteristics (Cui et al. 2003; Tang et al. 2009; Ni et al. 2014a, b; Ni 2015). Above a rainfall threshold, the saturation of pore-water pressure in the sedimentary matrix required for the initiation of a debris flow is attained (McCoy et al. 2012; Peruccacci et al. 2012).

The ratio of the time-scales of sediment renewal and strong rainfall events distinguishes between gullies with limited and unlimited sediment supply (Stiny 1910). This ratio is small in supply-unlimited gullies, where relatively weak intensity rainfalls and discharges are sufficient to trigger debris flows. The ratio is high in supply-limited gullies, where the sediment that has accumulated on the gully bed is transported during high-intensity rainfalls. Whether or not a debris flow will occur in a supply-limited gully mainly depends on the amount of sediment that has accumulated. If the amount of accumulated sediment is insufficient to initiate and sustain a debris flow, the sediment will be transported as fluvial bedload.

1.2: The Tongde sedimentary basin and the Daheba tributary

The present paper reports a field investigation on debris flows along the Daheba River, which is a tributary of the Yellow River in the incised Tongde sedimentary basin on the northeastern edge of the Tibetan Plateau (Fig. 1a). Wang et al. (2016, chapter 1.4) have introduced the Tongde sedimentary basin and the Daheba River. Moreover, they have analyzed the morphometry of the Daheba River and eleven of the major gullies. The main features will be summarized hereafter.

The Tibetan Plateau experiences uplifting and is simultaneously incised by rivers, providing favorable conditions for the onset of debris flows. Debris flows with volumes larger than one million cubic meters occur along the deeply incised valleys at the edge of Tibetan Plateau (Lyu et al., 2017a; Wang et al., 2016). The Tongde basin formed during the quaternary period (Craddock et al., 2010). It has an

90 average elevation of 330 m and a drainage area of 3,986 km^2. This basin is a graben basin where the
91 elevation is much lower than the surrounding mountains (Fig. 1b). A graben is defined as a depressed
92 segment of the earth bounded on at least two sides by faults. Pebbles, gravel, and sand accumulated in
93 the basin, forming a very thick sedimentary deposit (Fig. 1b). About 0.15 million years ago, the Yellow
94 River started incising in the sedimentary deposit of the Tongde basin (Fig. 1b; Li et al. 1996). The
95 incision progressed towards upstream from the Yellow River into its tributaries and induced the
96 development of new stream networks in the watersheds of these tributaries (Wang et al. 2016).
97 The confluence of the Daheba and Yellow River is at an altitude of 2684 m. The Daheba is ~ 160 km
98 long and its headwaters are at an altitude of ~ 5300 m. It has a drainage area of ~4000 km^2. Debris
99 flows mostly occur in environments with limited sediment supply, such as rocky mountainous
100 environments. A particularity of the Daheba watershed is that they occur in a sand-gravel mountainous
101 environment with quasi-unlimited sediment supply. The high erodibility of the Daheba watershed can
102 be attributed to the poor vegetation cover, which is due to the thin loess layer (Wang et al. 2016).
103 The development of debris flow is further favored by the upstream migrating incision of the Daheba
104 River. Several villages were located along the Daheba River in regions where no debris flows occurred
105 in the past. In the last 20 years, the region of active debris flows has migrated upstream and frequent
106 debris flows have buried houses, roads, farmlands and forests on the debris flow fan, and forced the
107 villagers to abandon their villages (Fig. 2).

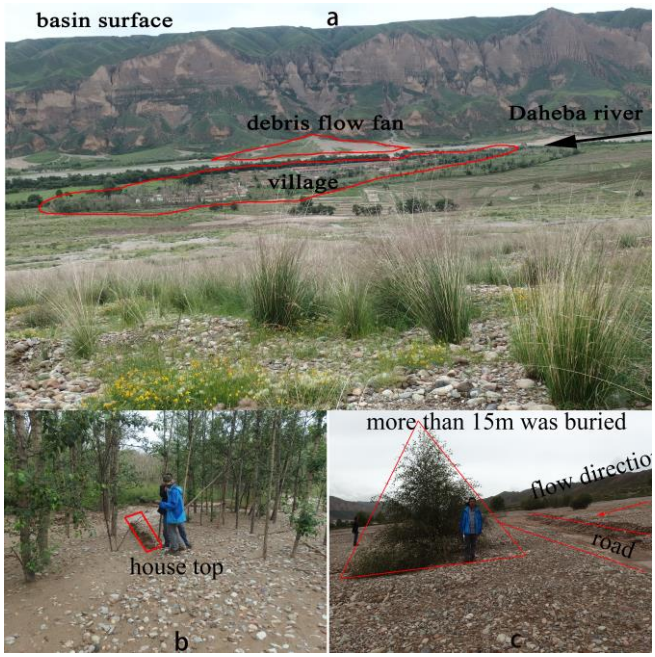

Figure 2. Debris flows deposition and its damage. (a) Villages buried by sediment deposition on the fan of the debris-flow gully at km 12.3; (b) House, road and trees buried by sediment deposition on the fan of the debris-flow gully at km 16.1

1.3: Objectives

The retrograding incision, frequent occurrence of debris flows and geological settings with quasi-unlimited sediment supply make the Daheba watershed an appropriate site for a field investigation on debris flows. As compared to the investigation of Wang et al. (2016), in the present paper all gullies in the watershed will be analyzed in detail, and hydro-sedimentary processes during individual debris-flow events will be investigated.

The objective of the investigation is to find answers to the following science questions:

(i) What are the main controls that determine whether or not debris flows will develop in a gully ? Or in other words: why do some gullies develop into debris-flow gullies and others not ?

(ii) What are the main hydro-sedimentary processes related to a single debris-flow event ?

(iii) How do gullies develop along the Daheba River due to debris flow events ?

(iv) What are the characteristics of the morphologically most active gullies ?

(v) How will the landscape and topography of the Daheba watershed evolve under the effect of debris

flows ?

2. Methods

A geophysical exploration was performed with an EH4 electromagnetic imaging system along the Daheba River at 20 km, 40 km, 68 km and 90 km upstream of its confluence with the Yellow River (Fig. 3). This exploration accurately provided the depth of the interface between sediment deposits and the underlying bedrock, the thickness of the sediment deposits, and the type of sediment. At the same locations, the incision depth of the Daheba River with respect to the basin surface was measured with a Kustom Signal LaserCam 4 LIDAR, with an accuracy of 0.1 m and a measurement range of 2,000 m. Additional data obtained with the same techniques at 2 km upstream of the confluence is taken from Wang et al. (2016).

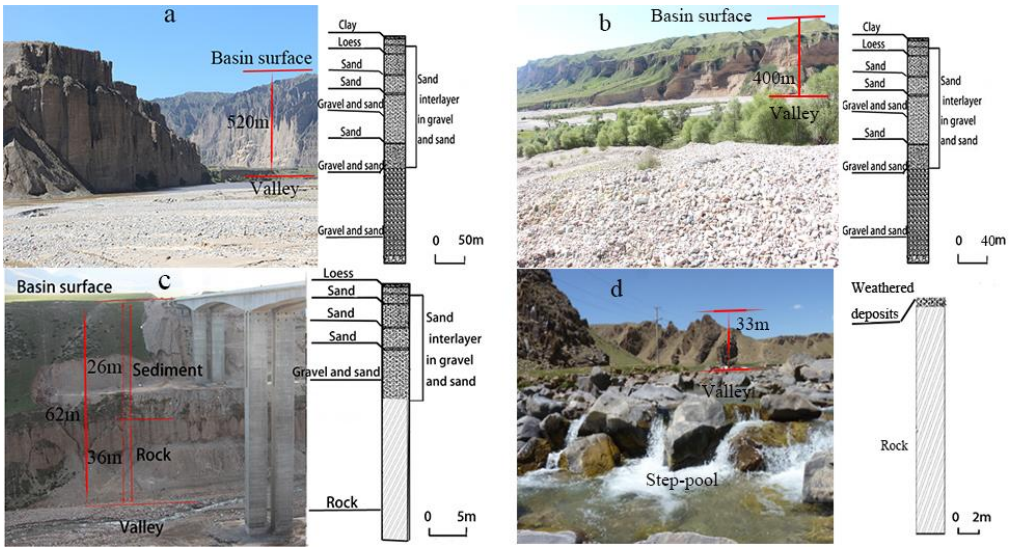

Figure 3. Pictures illustrating: (a) 520 m incision depth in the sediment deposition layer at km 2 in the sediment-basin reach; (b) 400 m incision depth in the sediment deposition layer at km 20 in the sediment-basin reach. (c) 62 m incision depth at km 40 in the transition reach, consisting of 26 m incision in the sediment deposition layer and 36 m incision in the underlying bedrock; (d) 33 m incision depth in the bedrock layer at km 90 in the mountain reach. The figures at the right of each picture illustrate the stratigraphy estimated from geophysical exploration.

A morphometric analysis of the Daheba watershed was based on a Digital Elevation Model (DEM) with a 10 m horizontal resolution, available from Lyu (2017a). For gullies with drainage area smaller

than 0.2 km^2 additional high-resolution topographic measurements with a grid size of 0.5 m were performed with a Trimble R8 RTK-GPS, with planimetric and altimetric accuracies of 0.01 m and 0.02 m, respectively. The software package ArcGis 10.1 was used to determine the hydrographic network of gullies that feed the Daheba River (Fig. 1c), and topographic characteristics such as the gullies' drainage area, cross-sectional shape, and longitudinal gradients of the gullies and fans (Table 1 as online supplementary material). A total number of 152 gullies were identified along the Daheba River. They are labeled with their distance in km from the confluence with the Yellow River. Gullies with accessible fans were then investigated in further detail.

The type of flow that shapes a gully leaves a clear footprint on the characteristics of the depositional fan (Hungr et al. 2001, Pederson et al. 2015). Debris-flow fans are shaped by deposition of many debris flow events. They predominantly consist of poorly sorted gravel, sand and fine particles, but large boulders and cobbles are typically present near the fan margins. Debris-flow fans are typically relatively steep (as quantified by the average gradient from the gully toe, which is also called fan apex, to the fan margin) and have sharp fan margins. Non-debris-flow fans can be shaped by floods only, or by the combined effect of floods and hyper-concentrated flow. Non-debris-flow fans are characterized by flatter fans and well-sorted sediment.

In order to characterize the gullies, the sediment on the depositional fan was analyzed for 122 gullies. Sediment samples were taken on a 10 m by 10 m grid in the center of the fan, and the sediment was divided into fine (0.1 to 1 mm), medium (1 to 10 mm) and coarse (10 to 50 mm) fractions (Table 1).

The spatial distribution of the gullies along the Daheba River was quantified by the number of gullies along 10 km long reaches of the Daheba River, called the distribution density. This distribution density was computed on a 5 km interval. The distribution density at km 40, for example, represents the

number of gullies in the reach from km 35 to km 45, divided by ten. The distribution density was computed for debris-flow gullies and non-debris-flow gullies separately.

Based on the laboratory work of Lyu et al. (2017b), the sediment eroded on the gully banks is expected to play an important role in the generation and the dynamics of debris flows. The amount of sediment available on the gully banks has therefore been estimated, according to a method introduced by Blothe et al. (2015) for estimating the volumes of potentially unstable rock mass. First, the excess volume, defined as the volume of erodible material located between the toe of the gully bank and an idealized topography with slope equal to the threshold hillslope angle S_t (Fig. 4), is computed. In the present analysis S_t = 30° has been adopted for granular sediment (sand and gravel) and bedrock has been considered as non-erodible, i.e. the excess volume excludes bedrock (Fig. 4). It should be noted that the separation between the sediment layer and the underlying bedrock is obvious and easily identifiable in gullies that are incised in the bedrock. Then, the excess topography Z_E is obtained by dividing the excess volume by the drainage area of the gully. The excess topography Z_E has been computed for each gully (Table 1). The computations were performed with the Matlab code developed by Li (2019).

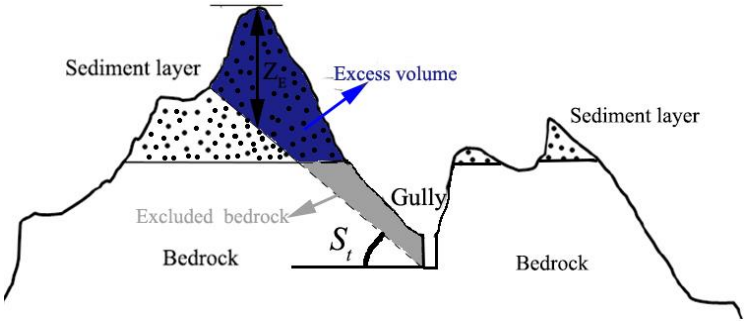

Figure 4. Excess volume, defined as the volume of erodible material located between the toe of the gully bank and an idealized topography with slope equal to the threshold hillslope angle St, excluding non-erodible bedrock. In the present analysis St = 30° has been adopted for granular sediment (sand and gravel). The excess topography ZE is obtained by dividing the excess volume by the drainage area of the gully. (Modified from Blothe et al. 2015).

The occurrence frequency of debris flows is important information. Debris-flow deposition has often

caused severe damage to agricultural fields, houses and other infrastructure located on the debris-flow fan (Fig. 2). The history of debris-flow events was estimated from interviewing local villagers. A total of 53 villagers were interviewed, leading to the identification of 614 debris flows in the last 20 years. In the end, only data of the last 10 years (2007-2017) were used to estimate the occurrence frequency. The information thus acquired provided estimates of the occurrence frequency in 50 gullies. Although the estimates are inherently rather inaccurate, they are sufficient for the purpose of the present investigation.

Debris flow events occurred on July 8th, 14th and 26th, 2016 (named event 1, 2 and 3 respectively) in the gully at km 11.4. The first debris flow event was recorded in the upper and middle reaches of the gully (Fig. 1c) at a frequency of 25 Hz with a hand-held camera. The videographies are available as online supplementary material. Characteristics of the debris flow dynamics were derived from the video analysis. In the middle reach of the gully, a Lagrangian analysis was adopted to track the velocity of the debris flow head (Fig.5 a-d). In the upper reach of the gully, an (approximate) Eulerian analysis was adopted to estimate the debris flow velocity, based on tracking tracers at the surface of the debris flow while it passes through the fixed cross-section 1-1 (Fig. 5e).

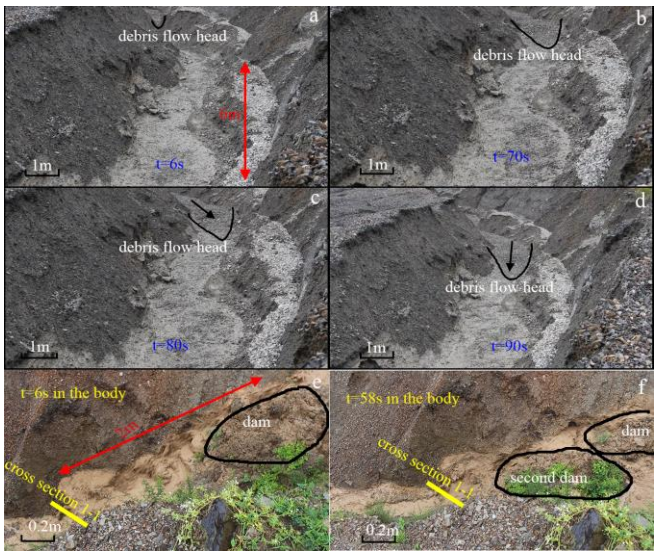

Figure 5. Snapshots from videography of the debris flow event on July 8, 2016 in the gully at km 11.4: (a-d) Lagrangian analysis of the motion of the debris flow head in the middle reach of the gully. (e-f) Euler analysis of debris flow body in cross section 1-1 in the upper reach of the gully. The locations of the images are shown in Figs. 1c and 11a. The videos are provided as online supplementary material.

In addition, the relation between the characteristics of the debris flow body and sediment supply from bank collapse were qualitatively analyzed from the videography. Figs. 5e,f, for example, illustrate bank collapse that leads to the formation of a barrier dam in the gully. The estimations of the velocities are approximate, but the accuracy is sufficient to provide insight in the dominant hydro-sedimentary dynamics of the debris flow.

The bed elevation changes induced by debris flow events 1 and 2 were estimated every 0.5 m along the entire gully axis by comparing longitudinal bed profiles measured with a Trimble R8 RTK-GPS before debris flow event 1, between events 1 and 2, and after event 2.

3. Field observations

3.1 Characteristics of the Daheba watershed and the debris-flow gullies

According to the geophysical exploration at km 2, 20, 40, 68, and 90, the sediment thickness was 650, 600, 26, 2, and 0 m, respectively, and the incision depth 520, 400, 62, 50, 33 m, respectively (Fig. 3, 6a). In the most downstream reach (km 2 and km 20), the deposits essentially consist of two layers: a pebble-sand layer at the basis and clay-loess layer on the top (Fig. 3a). At km 40 and further upstream, the Daheba River has cut through the sedimentary deposits and incised into the underlying bedrock. At km 40, the Daheba River has incised 36 m in the bedrock (Figs. 3b, 6a), and at km 68 even 48 m (Fig. 6a). As a result, the debris flow gullies have also incised in the bedrock, at least in their downstream parts. At km 68.5, for example, the gully has become funnel shaped and the incision depth in the bedrock illustrated in Fig. 6b is ~22 m. This funnel shape is the result of accelerated incision in the past thousand years: the top portion is the gradual incision zone and the lower portion is the rapid incision

zone (Wang et al. 2016). At km 71 and further upstream, there is no significant sedimentary deposit anymore, and the bedrock is weathered into poor-psephicity deposits of large size (Fig. 4d). Psephicity is the degree of roundness of the sediment particles. It increases along the flow direction due to abrasion and reflects the transport distance. The riverbed in this upstream reach has developed into a step-pool system typical of gravel-bed mountain rivers (Wang et. al 2016).

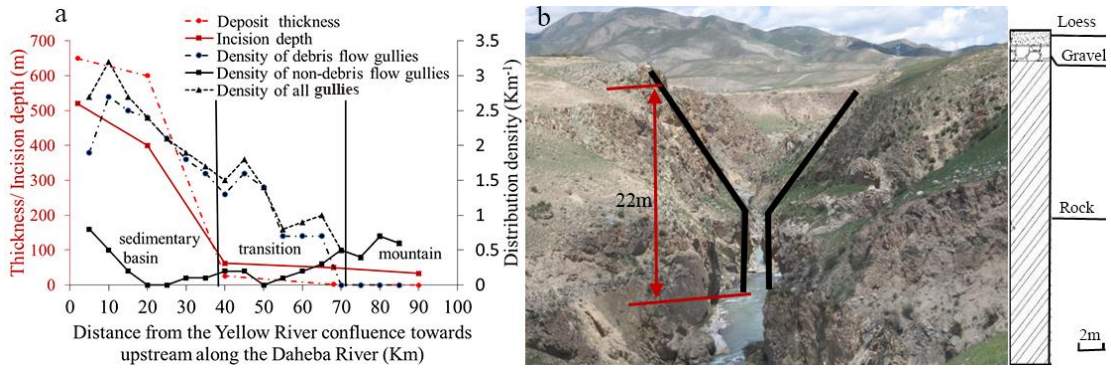

Figure 6. (a) Spatial evolution of the thickness of the sediment deposition layer and of the incision depth of the Daheba River (defined as the elevation difference between the surface of the sedimentary basin and the bottom of the Daheba River) (cf. Fig. 3). Distribution density (number of gullies per km length of the Daheba River) of debris-flow and non-debris-flow gullies along the Daheba River. (b) Funnel-shaped gully incised in the bedrock in the gully at km 68.5 (copyright Wang et al. 2016).

Among the 152 investigated gullies along the Daheba River, 114 were debris-flow gullies and 38 were non-debris-flow gullies. Their location along the Daheba River is indicated in Fig. 7. All of the gullies and their characteristics are given in Table 1. The fans of the debris-flow gullies typically had gradients in the range 0.10 - 0.30, whereas the non-debris-flow fans were much flatter with gradients in the range 0.01 - 0.07. Sediment compositions were also markedly different: poorly-sorted and coarser on the debris-flow fans vs. well-sorted and finer on the non-debris-flow fans. On the average, the sediment on debris-flow fans consisted of 58.9 % coarse sediments (10 to 50 mm), 23.4 % medium sediment (1 to 10 mm) and 17.8 % fine sediment (0.1 to 1 mm) with standard deviations of 4.5%, 2.5% and 5.3 %, respectively, and the sediment on non-debris-flow fans consisted of 12.1 % coarse sediments, 17.7 % medium sediment and 76.9 % fine sediment with standard deviations of 1.7%, 5.3% and 10.6 %,

respectively. Accumulations of coarse particles were observed in the lateral levees and frontal margins of all debris flow fans, whereas only well-sorted fine and medium particles were observed in the non-debris-flow fans. No clear relation between the sediment composition and the gully area is identifiable.

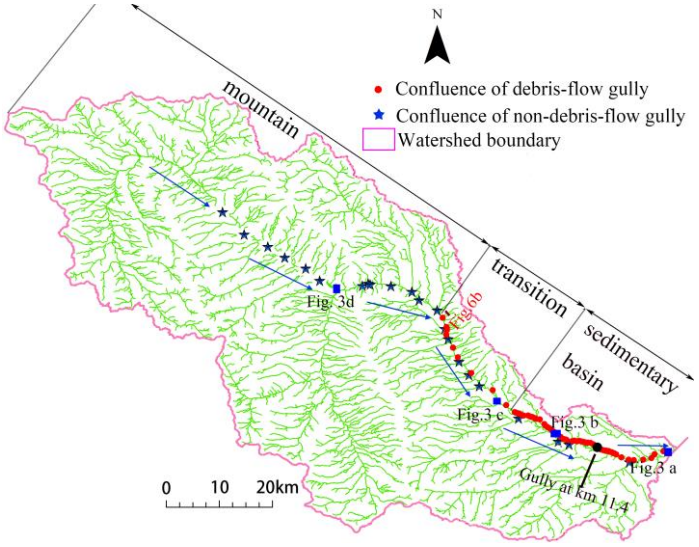

Figure 7. Distribution of the debris-flow and non-debris-flow gullies along the Daheba River. Separation of the Daheba River into three reaches: the sedimentary basin reach (km 0 - 38), the transition reach (km 38- 71), and the mountain reach (upstream of km 71).

The distribution density of the gullies is also shown in Fig. 6a. It reaches a maximum value of ~ 3 at km 10 and then steadily decreases to values of ~ 0.5 upstream of km 70. Near the confluence with the Yellow River, debris-flow gullies are dominant, but also non-debris-flow gullies occur. From km 10 to 50, the distribution density of debris-flow gullies is high and hardly any non-debris-flow gullies occur. Upstream of km 50, the distribution density of debris-flow gullies decreases and that of debris-flow gullies decreases. Upstream of km 70, only non-debris-flow gullies occur.

Wang et al. (2016) have separated the Daheba River into three reaches. The sedimentary basin reach is the reach in the Tongde basin where the river incision has not yet reached the base level of the deposited sediment, i.e. it has not yet incised in the underlying rock. The mountain reach is the reach outside the Tongde basin, i.e. the reach where there is no significant layer of deposited sediment

anymore. The transition reach is the reach in between where the river has reached the base level of the deposited sediment and is incising in the underlying rock. Based on the results of geophysical exploration, the classification of the gully type, and the gully distribution density, the three reaches can now accurately be located: the sedimentary basin reach from km 0 to km 38, the transition reach from km 38 to km 71 and, the mountain reach upstream of km 71 (Figs. 6, 7).

In the sedimentary basin reach, 81 debris-flow gullies and 11 non-debris-flow gullies occur. Seven of these non-debris flow gullies are within 7.5 km of the Yellow River confluence and have very small drainage areas (Table 1). The transition reach contains 33 debris-flow gullies and 6 non-debris-flow gullies, and the mountain reach 21 non-debris-flow gullies.

Figure 8 shows that the gully gradient tends to decay about logarithmically with increasing gully drainage area. The gully gradient can be steeper than 0.4 in the smallest gullies. Debris-flow gullies with such steep slopes generally have drainage areas that are an order of magnitude larger than non-debris-flow gullies with similar slopes. In general, however, this relation between gully gradient and drainage area is remarkably similar for debris-flow gullies and non-debris-flow gullies, and for gullies in the sedimentary basin, transition and mountain reaches.

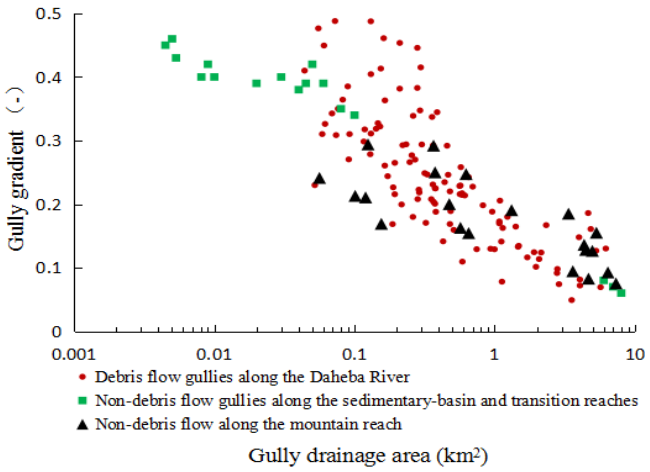

Figure 8. Gully gradient vs. gully drainage area for debris-flow and non-debris flow gullies along the Daheba River.

Fig. 9 shows the excess topography Z_E versus the gully drainage area for the debris-flow and non-debris-flow gullies. For debris-flow gullies, Z_E varies from 55 m to 367 m with an average value of 215 m, indicating that a large amount of sediment is available on the steep gully banks for fueling debris flows. The smallest values of Z_E are observed for the smallest (< 0.1 km^2) gully drainage areas. Z_E then increases about monotonically and values of Z_E > 250 m are found for gully drainage areas of intermediate size in the range 0.25 – 1.70 km^2. For larger drainage areas, Z_E decreases about monotonically and reaches a value of 62 m for the largest drainage area of 6.2 km^2. For non-debris-flow gullies, the largest observed excess topography is Z_E = 52 m. The average value in the intermediate reach is Z_E =25 m and in the mountain reach Z_E is by definition close to zero.

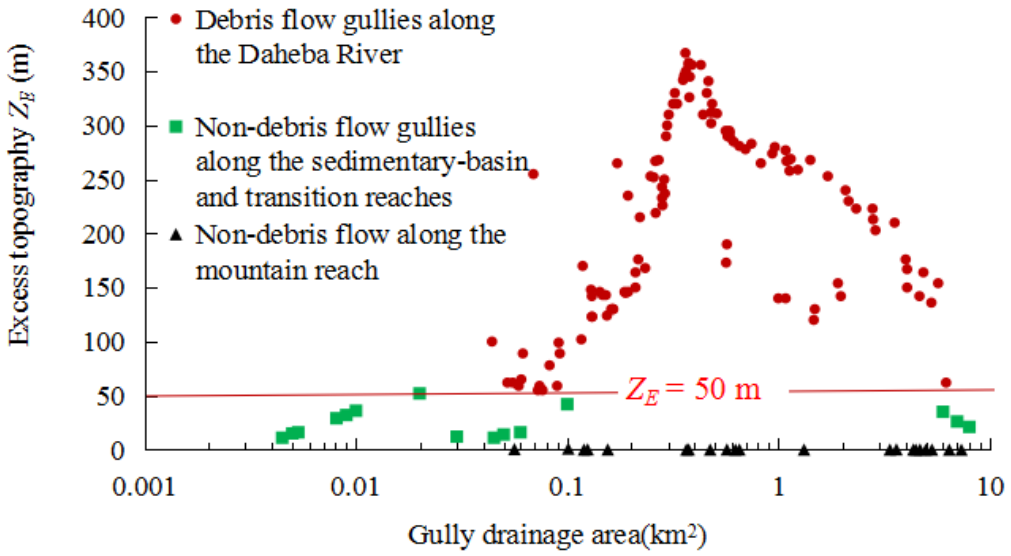

Figure 9. Excess topography Z_E (cf. Fig. 4) vs. gully drainage area for debris-flow and non-debris flow gullies along the Daheba River.

Not all debris-flow gullies are equally active. Figure 10 shows the occurrence frequency of debris flows, expressed as number of occurrences per year, versus the gully drainage area. No debris flows were reported in the smallest (< 0.045 km^2) and largest (> 5.3 km^2) gullies. Small (0.045-0.07 km^2) and large (2.2-5.3 km^2) gullies have the lowest frequency of debris flow outbreaks, with on the average less than one debris flow event every five years. In most gullies with a drainage area in the range 0.13-2.2

302 km^2, debris flows occur more than once every second year. The more active debris-flow gullies (on the
303 average more than one event per year) have typically an intermediate drainage area in the range of 0.35
304 km^2 to 0.70 km^2. The most active gullies have debris-flow events 2 to 3 times per year. Since gully
305 drainage area and gully gradient are related (Fig. 8), the most active gullies typically have intermediate
306 gradients in the range 0.20 – 0.35.

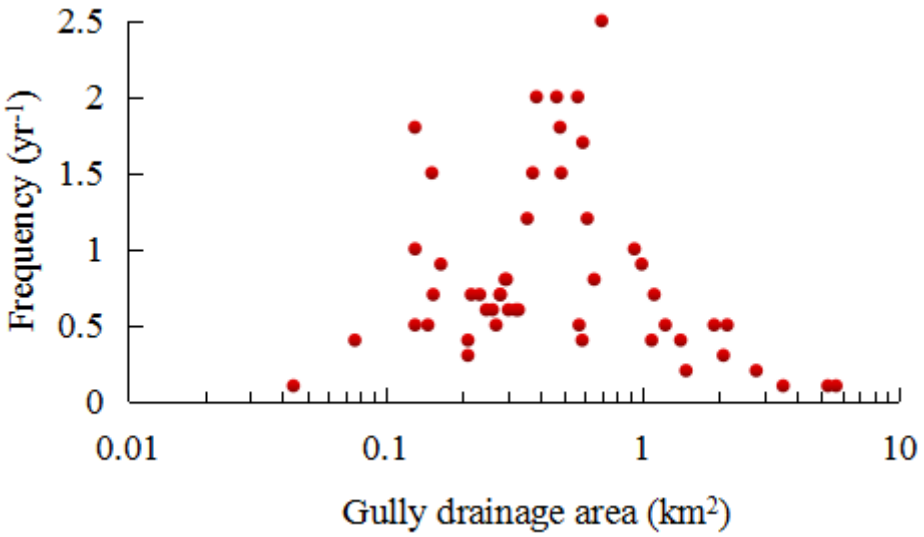

307 **Figure 10.** Occurrence frequency of debris flows vs. gully drainage area for
308 debris-flow gullies along the Daheba River.

309 Fig. 11 takes a closer look at the topography of one of the most active debris-flow gullies situated at
310 km 11.4. This gully, in which debris flow events have been monitored, has an area of 0.70 km^2 and an
311 average gradient of 0.23. According to Figure 10, this should be one of the most active debris-flow
312 gullies along the Daheba River, which is confirmed by the occurrence of 3 debris flows between July 8
313 and 26, 2016. The head of the debris-flow gully is steep and experiencing headward erosion (Fig. 11c).
314 The middle-reach of the debris flow gully is super V-shaped (Figs. 11 b,c). A super V-shaped gully
315 usually has steeper slopes in the lower parts than the upper parts of the banks, indicating accelerating
316 incision in the past (Wang et al., 2014). The bank slopes are significantly steeper than 30° (37°in
317 average with standard deviations of 2°), resulting in a large excess topography Z_E = 278 m (Table 1).

The gully's cross-sectional area increases in its upstream part, but then remains about constant in the middle-reach (Fig. 11b). The gully bed and banks are very irregular and rough (Fig. 11c). The cross-sectional shape on the fan is broad and concave (Figs. 11b, c), and the fan has a steep gradient of 0.15 (Table 1).

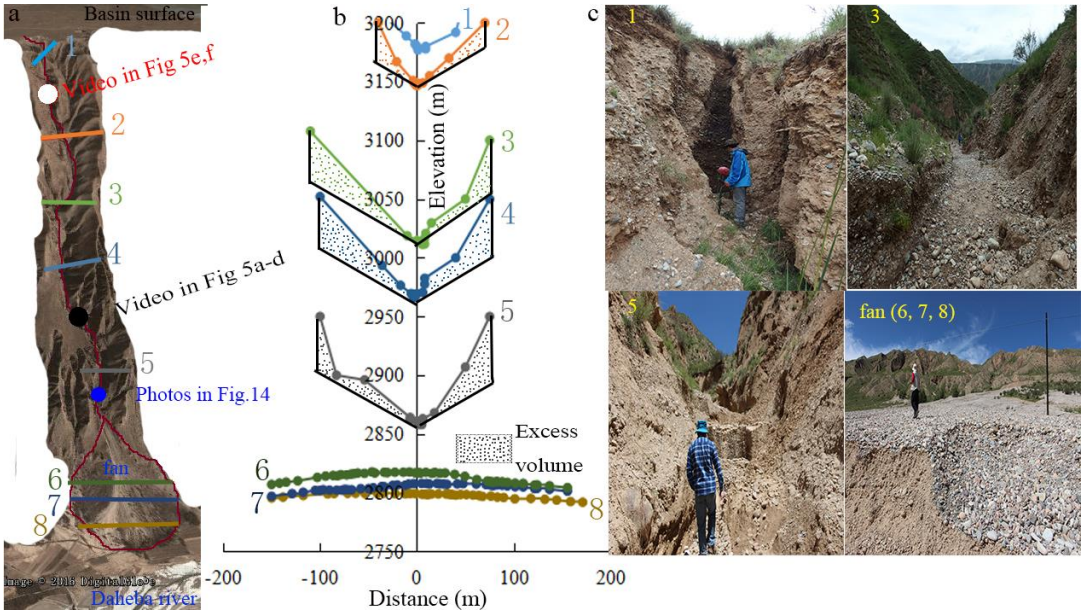

Figure 11. Topographic characteristics of the debris-flow gully at km 11.4 (cf. Figs. 1c, 5). (a) Detailed topography; (b) Cross-sectional shapes; (c) Pictures in selected cross-sections.

3.2 Flow and sediment dynamics of a debris flow event

Videography of the debris flow event that occurred on July 8, 2016 in this gully provides information on the dynamics of debris flows, including the characteristics of the flow, the erosion processes on the banks, the sediment flux in the gully, the changes in bed elevation and their interactions. Figure 12a shows the propagation velocity of the head of the debris flow in the middle reach of the gully at the location shown in Fig. 11a. The head enters the field of view of the camera after 6s (Fig. 5a). Initially, it has a propagation velocity of about 0.1 m s^{-1}. In the next minute, the head decelerates and ultimately comes to rest after about 66 s (Fig. 5b). At 79 s, the head is remobilized (Fig. 5c) and strongly accelerates to reach a propagation velocity of about 0.5 m s^{-1} (Fig. 5d). This intermittent motion of the

debris-flow head can be understood by considering the motion of the debris-flow body. Fig. 12b illustrates the velocity of the debris flow body in the upper reach of the gully at the location shown in Fig. 11a. The video sequence illustrates three remarkable features. First, the velocity of the debris-flow body is in general higher than that of the debris-flow head, implying that the debris-flow body continuously feeds the debris-flow head with sediment. Second, the velocity of the debris-flow body is intermittent and modulated by the intermittent sediment supply from bank collapse. Bank collapse leads to the formation of barrier dams in the gully, that cause a temporary partial (video sequences from 24-31 s, 47-65s and 67-97s) or total blockage (video sequence at 66s) of the debris flow. When these barrier dams break, bursts of high debris-flow velocity occur, which are called flood peaks (Figs. 5 e,f). Third, the dominant sediment supply to the debris flow comes from bank collapse.

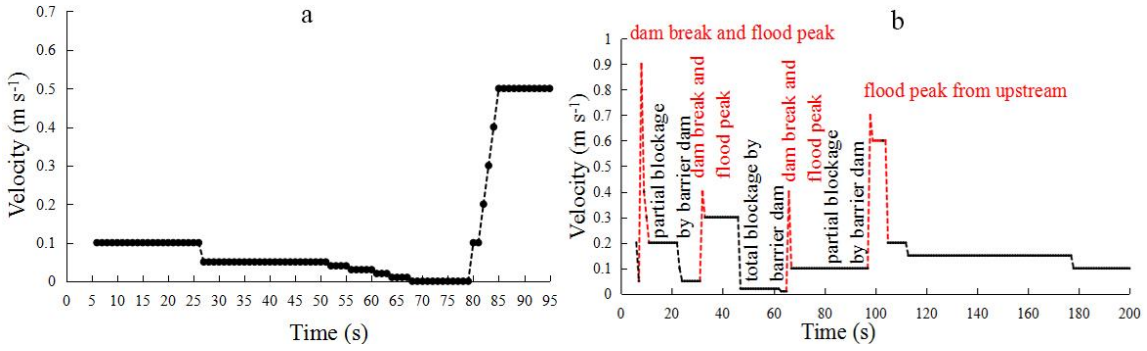

Figure 12. Characteristics of the debris-flow event that occurred on July 8, 2016 in the gully at km 11.4 (Figs. 1c, 5, 11a) estimated from videography (a) Velocity of the head of the debris-flow based on a Lagrangian analysis of the video taken in the middle reach of the gully. Note that the debris-flow enters the video image after 5 s and quits it after 95 s. (b) Velocity of the body of the debris flow while passing through section 1-1 (indicated in Fig. 5e,f) based on an Eulerian analysis of the video taken in the upper reach of the gully. The locations of the videography are shown in Figs. 1c and 11a. The video sequences are available as online supplementary material and representative snapshots are shown in Fig. 5.

Figure 13 shows the change in gully bed elevation induced by the debris flow events 1 and 2 on July 8 and 14, 2016, respectively. The debris flows caused a significant deposition of the order of 2 m on the gully fan (first 500 m from the Daheba River), where the gully slope flattens in downstream direction.

347 This confirms and explains the burial of houses and trees on a debris-flow fan illustrated in Fig. 2.

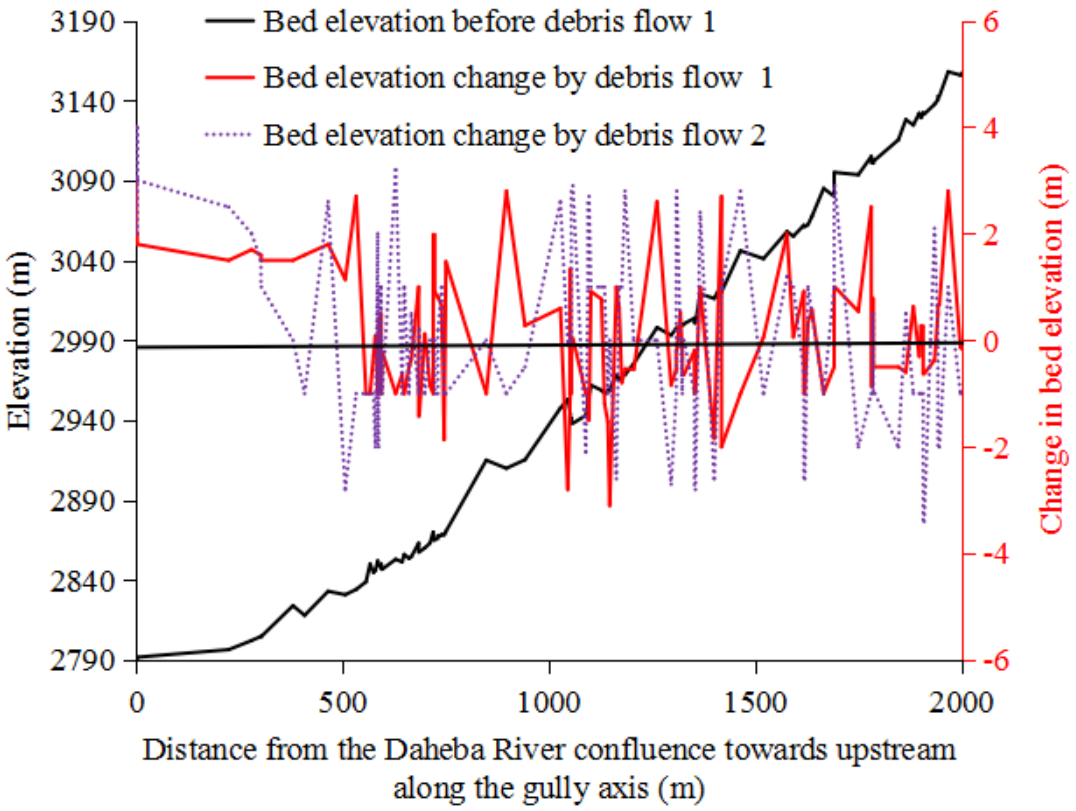

Figure 13. Longitudinal profile of the bed of the debris-flow gully at km 11.4 and changes in bed level elevation induced by debris flow event 1 on July 8, 2016 and 2 on July 14, 2016. The average incision of the gully excluding the depositional fan was 0.052 m for event 1 and 0.067 m for event 2.

348 Further upstream in the middle reach of the gully, the debris flows have caused alternating patterns of
349 erosion and deposition with amplitudes of up to 2 m. Both debris flow events have led to further
350 incision of the gully: the average incision induced by the first and second event were 0.052 m and
351 0.067 m, respectively. This indicates that the alternating patterns of erosion and deposition merely
352 represent debris-flow induced macroscale bedforms, such as barrier dams. More important, this
353 indicates that the important volume of transported sediment does not originate from the gully bed, but
354 essentially from bank erosion and collapse. Upstream of the gully fan, the gully slope is rather constant
355 on a macro-scale, but large steps of up to 10 m exist locally (Fig. 13). These large steps typically
356 represent barrier dams shaped by debris flow events.

Fig. 14 shows a location in the gully just upstream of the depositional fan (Fig. 11a) before and after the debris flow of July 8, 2016. Fig. 14 a, b illustrate that abundant sediment is available on the gully bed, which plays an important role in igniting debris flows. Sediment that is spread out over the gully bed mainly results from continuous small-scale bank erosion in the period between two debris flows (Fig. 14a). During debris-flows, this sediment is washed away, but immediately replaced by sediment supplied by bank collapse during the debris flow event (Fig. 14c). Barrier dams in the gully may result from debris flows, or may also be due to larger-scale bank collapse in the period between two debris flows (Fig. 14b). These barrier dams are not always completely washed out by debris flows, as illustrated in Fig. 14d.

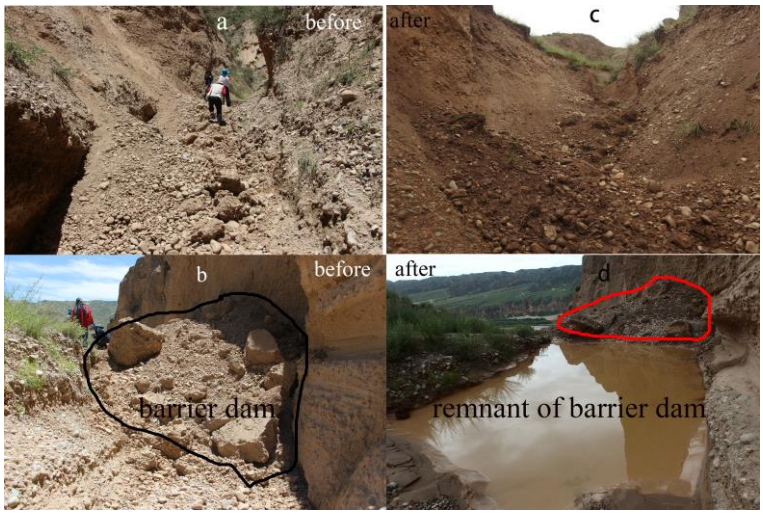

Figure 14. Gully morphology and sediment availability in the gully at km 11.4 at the location shown in Fig. 11a; (a,c) are upstream looking and (b,d) are downstream looking. The pictures compare the gully morphology before (a,b) and after (c,d) the debris-flow event of July 8, 2016. (a,c) Illustrate that there is always abundant sediment available on the gully bed in this supply-unlimited debris-flow gully. (b,c) Illustrate that large-scale barrier dams occur on the gully bed, and that they are not always entirely washed out by a debris-flow event.

4. Analysis, interpretation and discussion

The reported observations can be summarized in conceptual models for the hydro-sedimentary processes related to debris flows in supply-unlimited watersheds at different spatial and temporal scales:

a single-debris-flow event, the evolution of a single debris-flow gully, and the topographic evolution of the entire watershed. The science questions defined in Section 1.3 will now be revisited based on the observations.

4.1 Debris-flow gullies vs non-debris-flow gullies

The Daheba watershed has been divided into three reaches: a downstream sedimentary basin reach where debris flows are dominant, an upstream mountain reach where no debris flows occur, and an intermediate reach where both gullies with and without debris flows exist (Figs. 6, 7). Remarkably, debris-flow and non-debris flow gullies are characterized by a similar relation between gully drainage area and gully gradient (Fig. 8). In other words, the relation between gully drainage area and gradient cannot explain why debris flows develop in some gullies and not in others.

According to the observations, the availability of sediment, quantified by the excess topography Z_E (Figs. 4, 9), is the dominant factor that determines whether or not debris flows will develop in a gully. Sediment is abundantly available in the sedimentary basin reach where the Daheba River is incising in a thick sand-gravel layer, whereas hardly any sediment is available in the mountain reach, where the gullies are carved out in more erosion-resistant bedrock. For the Daheba River gullies, the threshold value of $Z_E \sim 50$ m seems to distinguish debris-flow and non-debris-flow gullies (Fig. 9).

Debris-flow gullies are supply-unlimited, i.e. they are continuously supplied with sediment from the steep erodible gully banks (Figs. 5e, 5f, 14). Similar supply-unlimited debris flows are known to occur in volcanic ash environments (Nocentini 2015). Non-debris-flow gullies are supply-limited. The low erodibility of the rocky gully banks prevents timely renewal of sediment on the gully bed, which is a requirement for sustaining debris flows. Glade (2005) has made similar observations in a low erodible rocky environment in Iceland, where two ten-year flood events occurred within 50 years. The first

flood triggered a debris flow because sufficient sediment was available in the gully, whereas the second did not because insufficient sediment had been replenished in the gully between the two floods.

4.2 Hydro-sedimentary processes of a supply-unlimited debris-flow event

Lyu et al. (2017b) have performed laboratory experiments to investigate the two main observations of the here-reported field investigation: the intermittent motion of the debris-flow, and the importance of sediment supply from bank collapse (Fig. 14a). Both are illustrated by the online supplementary movies. Based on the here-reported field investigation and the laboratory experiments of Lyu et al. (2017b), the hydro-sedimentary processes of debris flows in supply-unlimited gullies can be conceptualized as indicated in Figure 15.

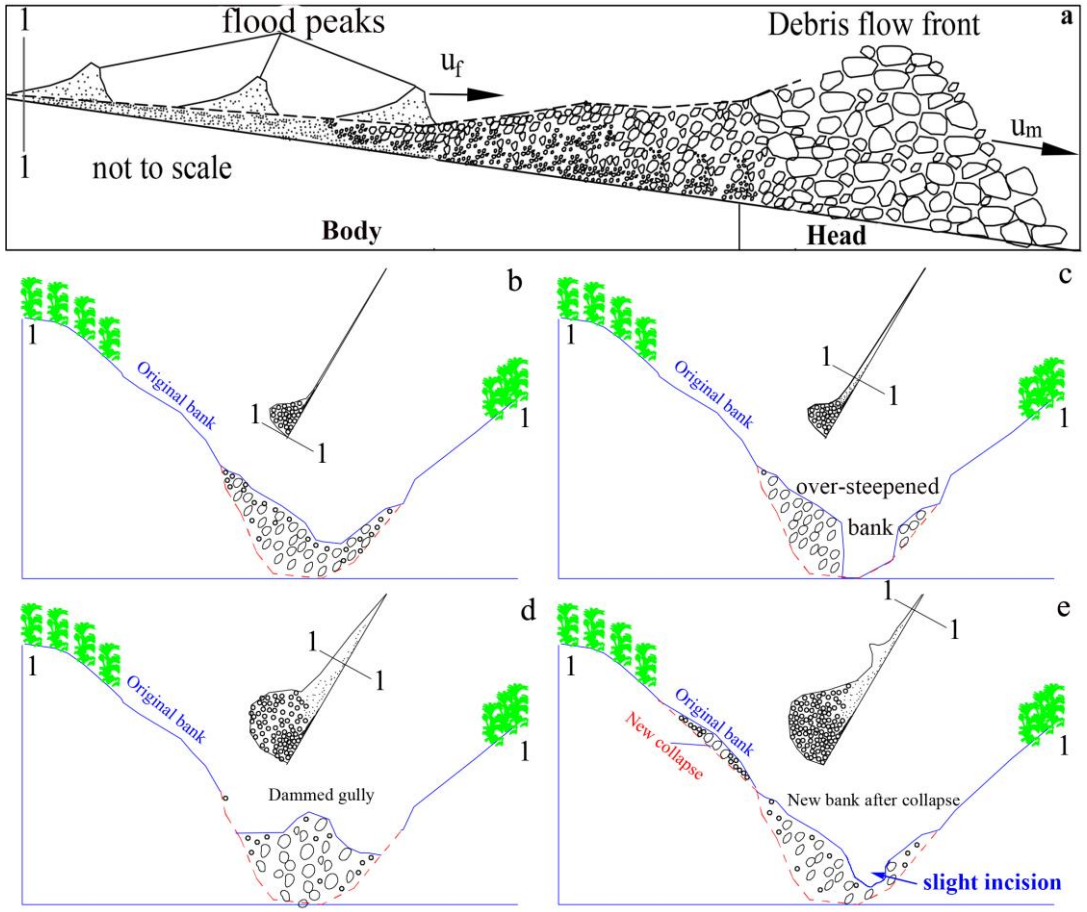

Figure 15. Conceptual model of hydro-sedimentary processes of debris-flows in supply-unlimited gullies. (a) Main features of a debris flow; (b-e) Sedimentary processes in the cross-section 1-1 induced by the passage of the debris flow.

Fig. 15a schematizes the main features of the debris flows. They consist of a coarse-grained head that is

404 followed by a body with finer sediment. The body generally moves faster than the head, $u_f > u_m$, which
405 is attributed to the sediment concentration that is considerably lower in the body than in the head,
406 leading to less resistance to flow. This implies that the body overtakes the head and constantly feeds it
407 with sediment, leading to the growth of the head.
408 The debris flow head evolves in an intermittent way (Fig. 12) due to a constant re-balancing of driving
409 and resisting forces. The growth of the head initially increases resisting forces and slows it down until
410 it comes to a rest. The body continues supplying sediment to the head, which continues growing. In
411 addition, water accumulates upstream of the head. At a threshold value for the size of the head, both
412 effects sufficiently increase the driving forces to remobilize the debris-flow head.
413 In between two debris-flow events, frequent small-scale bank erosion causes a deposition of sediment
414 on the gully bed (Fig. 15b). The debris-flow picks up of this sediment and erodes the gully bed (Fig.
415 15b,c). The sediment taken from the gully bed has two effects: it amplifies the growth of the
416 debris-flow head, and it creates an over-steepening of the bank near its toe (Fig. 15 c,d). The
417 over-steepened bank toe triggers additional intermittent bank collapses that supply sediment to the
418 gully. This sediment can form barrier dams that partially or totally block the gully (Figs. 5e,f, 14, 15d,
419 and movie in online supplementary material). In case of partial blockage, the barrier dam steers the
420 debris flow towards the opposite bank, thereby amplifying collapse of the opposite bank. Flood peaks
421 occur when these barrier dams collapse (Figs. 5, 15a,d,e). Because of their high velocities, these floods
422 peaks have a high capacity to transport sediment and to incise the bed.
423 The intermittent motion of the head of the debris flow and the intermittent development and collapse of
424 barrier dams leave a clear footprint on the gully morphology in the form of large-scale bedforms with
425 an amplitude of up to 10m in the Daheba watershed (Figs. 13, 14). The sediment transported by the

426 debris flow is deposited on the gully fan (Fig. 13). Although the debris flow causes further incision of
427 the gully bed (Fig. 13), the majority of transported sediment does not originate from the gully bed, but
428 from bank collapses. This is clearly illustrated by the gully at km 11.4: a single debris flow deposits a
429 layer of about 2 m thickness on the fan, but only leads to incision of the gully of about 0.05 m (Fig.
430 13).

431 4.3 Development of a supply-unlimited debris-flow gully and fan

432 It can reasonably be assumed that the growth rate of a supply-unlimited debris-flow gully (i.e. the
433 growth of the gully drainage area and the incision of the gully) depends on the occurrence frequency of
434 debris-flow events. The observations show a clear relation between the occurrence frequency of debris
435 flows (Fig. 10) and the sediment availability as expressed by the excess topography Z_E (Fig. 9): both
436 are small in the smallest gullies, increase to maximum values in gullies of intermediate size, which are
437 gullies with a drainage area of about 0.35 to 0.65 km^2 for the case of the Daheba River, and decrease
438 towards small values for larger gullies. Debris flows occur along the Daheba River in gullies spanning
439 a wide range of drainage areas (0.05 to 10 km^2) and gradients (0.05 to 0.5) (Fig. 8). When gullies form,
440 their area is small and their gradient is high (Fig. 8). No debris flows occur in the smallest gullies along
441 the Daheba River, typically with an area smaller than 0.1 km^2 in spite of their very steep slope (Fig. 8).
442 This is attributed to the low availability of erodible sediment (Fig. 9). When gullies and their drainage
443 area grow through bank erosion and bed incision, Z_E increases (Fig. 9) and allows for the development
444 of debris flows. With further growth of the gully drainage area, Z_E and the debris-flow frequency
445 increase (Figs. 9, 10), until they reach maximum values in gullies with a drainage area of intermediate
446 size. These are assumed to be the morphologically most active gullies with the highest growth and
447 incision rates. With further growth of the gully drainage area, Z_E (Fig. 9) and, in particular, the

448 debris-flow frequency decrease (Fig. 10), which can be attributed to the milder gully gradient, which
449 opposes the development of debris flows (Fig. 8). No debris flows were observed in the largest gullies
450 (Fig. 8).
451 The rather similar sediment composition on all debris-flow fans indicates that there is no noticeable
452 change in sediment composition during the development of gullies. This is explained by the fact that
453 the sediment originates from the same thick sandy-gravel deposition layer (Fig. 3).
454 The deposition on the fan gives an indication of the total volume of sediment transported by a debris
455 flow event. This total volume of transported sediment also seems to be related to Z_E. A debris flow
456 typically deposits a sediment layer of ~2m thick on the fan of the gully at km 11.4, which is
457 characterized by Z_E = 278 m. On the gully at km 16.1 characterized by Z_E = 190 m, the thickness of the
458 deposition layer is typically only 0.5 m. This value was estimated by excavating the depositional fan
459 over 6 m.
460 4.4 Morphological development of the Daheba watershed
461 The recent history of damaging sediment deposition on debris-flow fans (Fig. 2) suggests that the reach
462 of most active debris flows is migrating upstream in the Daheba watershed. The observations and the
463 conceptual model for the development of debris-flow gullies underpin this upstream migration.
464 Between km 0 and 5 and km 23 and 47, the gullies with the largest drainage area and the lowest
465 occurrence frequency of debris flows are observed (Fig. 16). This suggests that gullies in this reach are
466 at the end of their development stage after a previous stage of high rate of development. Gullies with
467 the highest occurrence frequency of debris flows and relatively small drainage area are found just
468 upstream of both reaches: between km 9 and 22 in the sedimentary basin reach and between km 45 and
469 68 at the upstream end of the intermediate reach (Fig. 16). These reaches are supposed to be in their

most active development stage. The lack of available sediment in the mountain reach will limit the further upstream migration of the reach of most active debris flows.

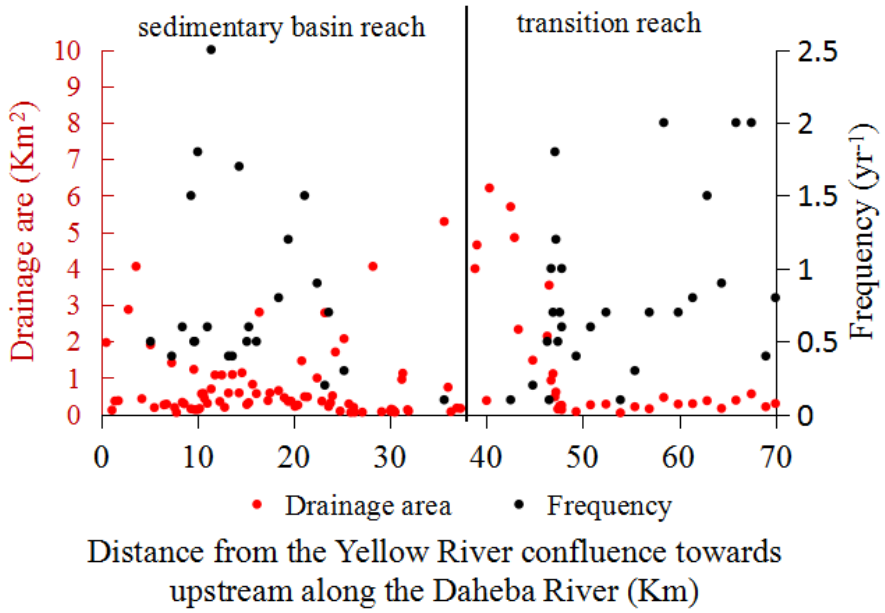

Figure16. Spatial evolution of the drainage area and the frequency of occurrence of debris flows in debris-flow gullies along the Daheba River.

These interpretations are in line with the findings of Wang et al. (2016). Based on an analysis of the shape of the longitudinal profile according to Jang (1987), they concluded that the sedimentary basin reach has already gone through the deep incision period and is now moving into a stable period, that the mountain zone is in the stable period that developed before the incision of the Yellow River started, and that the transition zone is currently in the deep incision and headcut period.

The conceptual models of the development of individual gullies and the morphological development of the watershed have a validity that goes beyond the case study of the Daheba watershed. Characteristic time and length scales are case dependent, however, and essentially relate to the erodibility and availability of the sediment. The highly erodible and abundantly available sediment in the Daheba watershed make for small areas of debris-flow gullies and high frequencies of occurrence up to several events per year. This contrast with rocky watersheds: Coe et al. (2003) found occurrence frequencies of

20 to 10000 years, which conforms with an occurrence frequency of about 70 years observed by Lyu et al (2017a) in the rocky watershed of the Nu River at the southern edge of the Tibetan plateau. Lyu et al. (2017a) also observed a minimal gully area for the onset of debris flows of about 1 km^2 in rocky environments, which is much larger than the 0.05 km^2 observed in the Daheba watershed. These results indicate that two different mechanisms of mass movement and landscape evolution occur along the edge of the Tibetan Plateau that range from frequent debris-flows in supply-unlimited erodible material to less frequent debris flows in supply-limited rocky material.

5. Conclusion

This paper reported a field study on 152 gullies along the Daheba River, which is a tributary of the Yellow River that is incising in the Tongde sedimentary basin, situated on the northeastern edge of the Tibetan Plateau (Figs. 1, 7).

The field study includes a geophysical exploration of the subsurface of the Daheba watershed (Figs. 3,6), morphometric and sedimentologic analyses of the gullies (Figs. 4,8,9,11 and Table 1), estimations of the frequency of occurrence of debris flows in the gullies (Fig. 10), and characterizations of the hydro-sedimentary processes of individual debris flow events (Figs. 5, 12-15).

Debris flows occur in 114 gullies along the Daheba River (Fig. 7). The dominant control parameter for the occurrence of debris flow is the sediment availability in the gully drainage area, as parameterized by the excess topography Z_E. (Figs. 4,9) Debris flows develop in gullies with an excess topography above a critical threshold value, which is about Z_E = 50 m for the Daheba watershed (Fig. 9). Debris-flows in the Daheba watershed are supply-unlimited, i.e sediment is abundantly available from the steep erodible gully banks.

Debris flow consist of a head and body, which both move in an intermittent way (Figs. 12,15). The

508 body constantly overtakes the head (Fig. 12) and supplies it with additional sediment. The sediment in
509 the body mainly originates from bank collapse (Fig. 5,13, 14). The supplied sediment can temporarily
510 build barrier dams, which partially or totally dam the gully and cause a transient retention of the debris
511 flow (Figs. 5, 14). The barrier dam grows due to the supply of sediment from upstream and ultimately
512 breaks, leading to a so-called flood peak in the debris flow body (Figs. 5,15). Similarly, the constant
513 supply of sediment from the debris-flow body to the head makes it grow. Initially, this increases flow
514 resistance and slows down the head. When the head reaches a critical size, it is remobilized (Figs. 5,12).
515 The debris flow deposits on the fan (Figs. 2,13). Although the main sediment supply is provided by
516 bank collapse, debris-flow events also incise the gully bed (Fig. 13).
517 The growth and incision of debris-flow gullies in supply-unlimited watersheds is mainly controlled by
518 the frequency of occurrence of debris flows (Fig. 10), which is closely related to the excess topography
519 Z_E (Fig. 9). When gullies form, there is not yet enough sediment available to initiate and sustain debris
520 flows. When gullies and their drainage area grow through bank erosion and bed incision, Z_E increases
521 (Fig. 9) and allows for the development of debris flows. With further growth of the gully drainage area,
522 Z_E and the debris-flow frequency increase, until they reach maximum values in gullies with a drainage
523 area of intermediate size (Figs. 9, 10). These are assumed to be the morphologically most active gullies
524 with the highest growth and incision rate. With further growth of the gully drainage area, Z_E (Fig. 9) the
525 debris-flow frequency decrease (Fig. 10), which can be attributed to the milder gully gradient, which
526 opposes the development of debris flows (Fig. 8). No debris flows were observed in the largest gullies
527 (Fig. 8).
528 The Daheba watershed is divided into three reaches (Figs. 6,7). The sedimentary basin reach
529 downstream is the reach in the Tongde basin where the river incision has not yet reached the base level

530 of the deposited sediment, i.e. it has not yet incised in the underlying bedrock. The mountain reach is
531 the reach outside the Tongde basin, i.e. the reach where there is no significant layer of deposited
532 sediment anymore. The transition reach is the reach in between where the river has reached the base
533 level of the deposited sediment and is incising in the underlying rock. Debris flows are dominant in the
534 sedimentary basin reach, where Z_E is large, and no debris flows occur in the mountain reach where Z_E
535 is negligible. Both gullies with and without debris flows occur in the intermediate reach.
536 Gullies in the sedimentary basin reach typically have the largest drainage area and the lowest
537 occurrence frequency (Fig. 16), suggesting that they are at the end of their development stage after a
538 previous stage of high growth rate. Gullies in the transition reach typically have the highest occurrence
539 frequency and relatively small drainage areas, indicating that they are in their most active growth stage.
540 These observations confirm the upstream migrating incision of the Daheba watershed inferred by Wang
541 et al. (2016) based on an analysis of the shape of the longitudinal profile according to Jang (1987). The
542 lack of available sediment in the mountain reach will limit the further upstream migration of the reach
543 of most active debris flows.

544 **Online supplementary material**

545 Two movies illustrate the hydro-sedimentary processes of a supply-unlimited debris flow event. Both
546 movies are made in the gully at km 11.4 during the debris flow event on July 8, 2016.

547 Daheba_Gully11.4_UpperReach_HydrosedimentaryProcesses.mov

548 This 8 min 19s sequence is taken in the upper reach of the gully at the location indicated in Figs. 1c and
549 11a. The sequence clearly illustrated the main features of the hydro-sedimentary processes: the
550 sediment that is predominantly supplied by bank erosion, the formation and rupture of barrier dams that
551 partially or totally block the cross-section, the intermittent character of the processes.

552 Figure 12b is based on an (approximate) Eulerian analysis of the motion across section 1-1 (indicated
553 in Fig. 5e) in the 200 s time window from 0 min 5 s to 3 min 20 s. Figs. 5e,f show snapshots after 6s
554 and 58s in this time window.

555 Daheba_Gully11.4_MiddleReach_HydrosedimentaryProcesses.mov

556 This 1 min 35s sequence is taken in the middle reach of the gully at the location indicated in Figs. 1c
557 and 11a. The sequence clearly illustrated intermittent behavior of the head of the debris flow. Figure
558 12a is based on an (approximate) Lagrangian analysis of the motion of the head. Figs. 5 a-d show
559 snapshots after 6s, 70s, 80s and 90s in this time window.

560 **Acknowledgements**

561 Datasets for this research are available in these in-text data citation references: Wang et al. (2016),
562 [with this license, and these access restrictions if any], Li (2019) [with this license, and these access
563 restrictions if any].This study is supported by the National Natural Science Foundation of China
564 (41790434), the Second Tibetan Plateau Scientific Expedition and Research Program (2019QZKK0903)
565 and the National Natural Science Foundation of China (41907229, 41941019). Blanckaert as a visiting
566 professor of Tsinghua university is funded by the State Key Laboratory of Hydroscience and
567 Engineering Project (2019-KY-01).

568 **References**

569 Berger C, McArdell BW, Schlunegger F (2011) Direct measurement of channel erosion by debris flows,
570 Illgraben, Switzerland. J. Geophys. Res. Earth Surf. 116, F01002.
571 https://doi.org/10.1029/2010JF001722.

572 Bertrand M, Liébault F, Piégay H (2013) Debris-flow susceptibility of upland catchments. Nat Hazards
573 67:497-511

574 Blothe J H, Korup O, Schwanghart W (2015) Large landslides lie low: Excess topography in the
575 Himalaya-Karakoram ranges. Geology, 43(6):523-526. https://doi.org/10.1130/G36527.1
576 Ciurean RL, Hussin HY, van Westen C, Jaboyedoff M, Nicolet P, Chen L, Frigerio S, Glade T (2017)
577 Multi-scale debris flow vulnerability assessment and direct loss estimation of buildings in the
578 Eastern Italian Alps. Natural Hazards, 85: 929-957. https://doi.org/10.1007/s11069-016-2612-6
579 Coe JA, Godt JW, Parise M, Moscariello A (2003) Estimating debris-flow probability using fan
580 stratigraphy, historic records, and drainage-basin morphology, Interstate 70 highway corridor,
581 central Colorado, USA. In: Rickenmann D, Chen C (eds) Proc 3rd Int Conf on Debris Flow
582 Hazard Mitigation: Mechanics, Prediction, and Assessment, Davos 2:1085-1096.
583 https://www.researchgate.net/publication/235699081
584 Craddock WH, Kirby E, Harkins NW, Zhang H, Shi X, Liu J (2010) Rapid fluvial incision along the
585 Yellow River during headward basin integration. Nat Geosci 3(3): 209.
586 https://doi.org/10.1038/ngeo777
587 Cui P, Yang K, Chen J (2003) Relationship between occurrence of debris flow and antecedent
588 precipitation: taking the Jiangjia Gully as an example, China. J. Soil Water Conservation, 1:
589 11-15 (in Chinese)
590 Glade T (2005) Linking debris-flow hazard assessments with geomorphology. Geomorphology 66(1-4):
591 189-213. https://doi.org/10.1016/j.geomorph.2004.09.023
592 Godfrey A, Ciurean RL, van Westen CJ, Kingma NC, Glade T (2015) Assessing vulnerability of
593 buildings to hydro-meteorological hazards using an expert based approach-An application in
594 Nehoiu Valley, Romania. International Journal of Disaster Risk Reduction, 13:229-241.
595 https://doi.org/10.1016/j.ijdrr.2015.06.001.

596 Griffiths MD (1996) Behavioural addictions: An issue for everybody? Journal of Workplace Learning,
597 8(3): 19-25.
598 Hungr O, Evans SG, Hutchinson I (2001) A review of the classification of landslides of the flow type.
599 Environ Eng Geosci 7(3):221-238. http://discovery.ucl.ac.uk/id/eprint/1313933
600 Imaizumi F, Sidle RC, Tsuchiya S, Ohsaka O (2006) Hydrogeomorphic processes in a steep debris
601 flow initiation zone. Geophys. Res. Lett. 33: L10404. https://doi.org/10.1029/2006GL026250.
602 Iverson RM (1997). The physics of debris flows. Reviews of Geophysics, 35(3), 245-296.
603 Jang ZX (1987) Model of development and rule of evolution of the longitudinal profiles of the valley
604 of three rivers in the northwestern part of Yunnan province. Journal of Geographical Sciences,
605 42(1):16-27 (in Chinese).
606 Johnson CG, Kokelaar BP, Iverson RM, Logan M, LaHusen RG, Gray J (2012) Grain-size segregation
607 and levee formation in geophysical mass flows J. Geophys. Res., 117: F01032
608 Jomelli V, Brunstein D, Grancher D, Pech P (2007) Is the response of hill slope debris flows to recent
609 climate change univocal? A case study in the Massif des Ecrins (French Alps) Climate Change,
610 85:119-137
611 Kattel P, Khattri KB, Pokhrel PR, Kafle J, Tuladhar BM, Pudasaini SP (2016). Simulating glacial lake
612 outburst floods with a two-phase mass flow model. Ann. Glaciol. 57 (71): 349-358.
613 https://doi.org/10.3189/2016AoG71A039
614 Kovanen DJ, Slaymaker O (2008) The morphometric and stratigraphic framework for estimates of
615 debris flow incidence in the North Cascades foothills, Washington State. Geomorphology
616 99:224-245

617 Li JJ, Fang XM, Ma HZ (1996) The evoltion of the Yellow river geomorgraphy and the uplift of
618 Tibetan plateau. Science in China. 26(4): 316-322 (in Chinese).
619 Li Xin (2019) Debris Flow Risk Assessment Based on Negative Feedback of Barrier Dams and Excess
620 Energy. Master's dissertation, Tsinghua University, Beijing:30-31 (in Chinese)
621 Lorente A, Garcıa-Ruiz JM, Beguerıa S, Arnaez J (2002) Factors explaining the spatial distribution of
622 hillslope debris flows, A case study in the Flysch Sector of the Central Spanish Pyrenees,
623 Mountain Research and Development. 22:32-39
624 Luna BQ, Remaître A, Van Asch TWJ, Malet JP, VanWesten CJ (2012) Analysis of debris flow
625 behavior with a one dimensional run-out model incorporating entrainment. Eng. Geol. 128:
626 63-75. https://doi.org/10.1016/j.enggeo.2011.04.007
627 Lyu LQ (2016) Mechanism of the intermittent motion of two-phase debris flows. Environmental Fluid
628 Mechanics 17(1), 139-158.
629 Lyu LQ (2017a) Research on the initiation and motion of gully debris flows in Tibetan Plateau.
630 Doctoral dissertation, Tsinghua University, Beijing: 20 (in Chinese)
631 http://cdmd.cnki.com.cn/Article/CDMD-10003-1018876137.htm
632 Lyu LQ, Wang ZY, Cui P, Xu MZ (2017b) The role of bank erosion on the initiation and motion of
633 gully debris flows. Geomorphology 285: 137-151.
634 https://doi.org/10.1016/j.geomorph.2004.09.023
635 McCoy SW, Kean JW, Coe JA, Tucker GE, Staley DM, Wasklewicz TA (2012) Sediment entrainment
636 by debris flows: in situ measurements from the headwaters of a steep catchment J. Geophys.
637 Res., 117

638 Ni HY, Zheng WM, Song Z (2014a) Catastrophic debris flows triggered by a 4 July 2013 rainfall in
639 Shimian, SW China: formation mechanism, disaster characteristics and the lessons learned.
640 Landslides 11:909-921
641 Ni HY, Tang C, Zheng WM et al (2014b) An overview of formation mechanism and disaster
642 characteristics of post-seismic debris flows triggered by subsequent rainstorms in Wenchuan
643 earthquake extremely stricken areas. Acta Geol Sin-Engl 88(4):1310-1328
644 Ni HY (2015) Experimental study on initiation of gully-type debris flow based on artificial rainfall and
645 channel runoff. Environ Earth Sci 73:6213-6227
646 Nocentini, M., Tofani, V., Gigli, G (2015) Landslides, 12: 831.
647 https://doi.org/10.1007/s10346-014-0524-7
648 Papathoma-Köhle M, Keiler M, Totschnig R, Glade T (2012) Improvement of vulnerability curves
649 using data from extreme events: debris flow event in South Tyrol. Nature Hazards Earth Syst.
650 64: 2083-2105. https://doi.org/10.1007/s11069-012-0105-9.
651 Pederson CA, Santi PM, Pyles DR (2015) Relating the compensational stacking of debris-flow fans to
652 characteristics of their underlying stratigraphy: Implications for geologic hazard assessment and
653 mitigation. Geomorphology 248:47-56. https://doi.org/10.1016/j.geomorph.2015.06.030
654 Peruccacci S, Brunetti MT, Luciani S, Vennari C, Guzzetti F (2012) Lithological and seasonal control
655 on rainfall thresholds for the possible initiation of landslides in central Italy. Geomorphology,
656 139-140: 79-90. https://doi.org/10.1016/j.geomorph.2011.10.005.
657 Pudasaini S P. A general two-phase debris flow model. Journal of Geophysical Research: Earth Surface,
658 2012, 117(F3).

659 Reichenbach P, Busca C, Mondini AC, Rossi M (2014) The influence of land use change on landslide
660 susceptibility zonation: the Briga catchment test site (Messina, Italy) Environ. Manag., 54 (6):
661 1372-1384. https://doi.org/10.1007/s00267-014-0357-0
662 Suwa H (1988) Focusing mechanism of large boulders to a debris-flow front. Geomorphology:
663 151-178
664 Stiny J (1910) Debris flow. Wagnerschen Univ., Innsbruck
665 Tang C, Zhu J, Li WL (2009) Rainfall-triggered debris flows after Wenchuan earthquake Bull. Eng.
666 Geol. Environ., 68:187-194
667 Takahashi T (2009) A review of Japanese debris flow research. International Journal of Erosion
668 Control Engineering 2 (1): 1-14. https://doi.org/10.13101/ijece.2.1
669 Theule JI, Li'ebault F, Loye A, Laigle D, Jaboyedoff M (2012) Sediment budget monitoring of
670 debris-flow and bedload transport in the Manival Torrent, SE France. Nat. Hazards Earth Syst.
671 Sci. 12: 731-749. https://doi.org/10.5194/nhess-12-731-2012.
672 Wang ZY, Lee JHW, Melching CS (2014) River Dynamics and Integrated River Management.
673 Springer Verlag and Tsinghua Press, Berlin and Beijing, pp 134-135.
674 https://link.springer.com/content/pdf/10.1007%2F978-3-642-25652-3
675 Wang ZY, Li ZW, Xu MZ, and Yu G (2016) River morpho dynamics and stream ecology of the
676 Qinghai-Tibetan Plateau. CRC Press, Balkema.
677 https://www.researchgate.net/publication/310952767
678 Wang ZY, Wang GQ, Liu C (2005) Viscous and two-phase debris flows in southern China's Yunnan
679 plateau. Water Int. 30 (1): 14-23. https://doi.org/10.1080/02508060508691832

680 Wang ZY, Wai OWH and Cui P.. Field investigation on debris flows. International Journal of Sediment
681 Research, 1999, 14(4):10-23 Xu Q, Zhang S, Li W L, Asch TWJ (2012) The 13 August 2010
682 catastrophic debris flows after the 2008 Wenchuan earthquake, China. Natural Hazards and
683 Earth System Sciences, 12: 201-216. https://dspace.library.uu.nl/handle/1874/280990
684 Winter MG, Smith JT, Fotopoulou S, Pitilakis K, Mavrouli O, Corominas J, Agyroudis S (2013) The
685 physical vulnerability of roads to debris flow. Delage P, Desrues J, Frank R, Puech A, Schlosser
686 F (Eds.), Proceedings of the 18th International Conference on Soil Mechanics and Geotechnical
687 Engineering, Presses des Ponts, Paris, 2281-228
688 Zhou SY, Gao L, Zhang LM (2019) Predicting debris-flow clusters under extreme rainstorms: a case
689 study on Hong Kong Island. Bull Eng Geol Environ 78: 5775-5794.
690 https://doi.org/10.1007/s10064-019-01504-3

Table 1 Characteristics of the debris-flow and non-debris flow gullies and fans in the Daheba watershed

Distance from the confluence (km)	Latitude (°)	Longitude (°)	Gully drainage area (km^2)	Gully gradient	Fan gradient	Excess topography Z_E (m)	Frequency (yr^{-1})	Sediment size		
								5-1cm (%)	1-0.1cm (%)	0.1-0.01cm (%)
0.5	35.52068	100.14146	1.9711	0.101	0.113	142				
1.1	35.51956	100.13541	0.1166	0.298	0.224	102				
1.4	35.51873	100.13333	0.3661	0.204	0.174	346				
1.76	35.51684	100.12984	0.3751	0.201	0.120	356				
2.26	*100.1363*	*35.519809*	*0.0090*	*0.420*	*0.009*	*32*		*11*	*23*	*66*
2.33	*100.139*	*35.52068*	*0.0200*	*0.390*	*0.016*	*52*		*11*	*24*	*65*
2.41	*100.1371*	*35.520202*	*0.0100*	*0.400*	*0.018*	*36*		*12*	*34*	*54*
2.5	*100.1307*	*35.519517*	*0.0081*	*0.400*	*0.036*	*29*		*12*	*21*	*67*
2.6	*100.1141*	*35.505062*	*7.0000*	*0.070*	*0.035*	*26*		*13*	*11*	*76*
2.8	35.51718	100.1237	2.8755	0.074	0.105	203		63	26	11
3.6	35.51241	100.1088	4.0570	0.081	0.103	167		64	25	11
4.2	35.51493	100.10106	0.4289	0.141	0.127	356				
5.1	35.50303	100.0897	1.9098	0.124	0.106	154	0.5	63	23	14
5.5	35.50301	100.08299	0.1868	0.169	0.220	146				
6.5	35.50228	100.0735	0.2612	0.180	0.207	267		60	22	18
6.77	35.50289	100.07033	0.2825	0.208	0.163	226				
6.9	*100.0694*	*35.505215*	*0.0053*	*0.430*	*0.054*	*16*		*15*	*25*	*60*
7.2	*100.0664*	*35.505379*	*0.0050*	*0.460*	*0.064*	*15*		*14*	*24*	*62*
7.3	35.50294	100.0649	1.4138	0.165	0.107	268	0.4	61	26	13
7.3	*100.0653*	*35.505673*	*0.0045*	*0.450*	*0.052*	*11*		*12*	*23*	*65*
7.6	35.50573	100.05984	0.1888	0.226	0.030	145				
7.8	35.50629	100.05814	0.0521	0.230	0.355	62				
8.4	35.50679	100.0528	0.3308	0.247	0.182	320	0.6	60	24	17
8.6	35.50355	100.04383	0.2898	0.218	0.165	237				
9.3	35.51199	100.044	0.1522	0.322	0.207	143	1.5	59	23	18
9.6	35.51331	100.0411	1.2334	0.180	0.127	259	0.5	58	23	19
9.7	35.51397	100.0396	0.1309	0.404	0.247	123	0.5	57	23	20
10	35.51526	100.037	0.1307	0.488	0.257	142	1.8	57	22	21
10.2	35.51621	100.0344	0.1615	0.461	0.277	130		56	22	22
10.4	35.51666	100.0323	0.5647	0.216	0.123	173		55	22	23
10.6	35.51772	100.0309	0.5737	0.258	0.143	290		54	21	24
10.7	35.51751	100.0296	0.4394	0.235	0.182	310		53	21	26
11	35.51838	100.0264	0.3022	0.294	0.324	310	0.6	53	21	27
11.4	35.51917	100.0219	0.6972	0.227	0.153	278	2.5	52	21	28
11.8	35.52044	100.0181	1.0799	0.173	0.115	140		51	20	29
12.3	35.52334	100.0132	0.3532	0.208	0.192	342		50	20	30
12.5	35.52366	100.0106	1.0798	0.170	0.145	277		49	20	31
12.8	35.52571	100.0076	0.1939	0.265	0.227	146		49	19	32

Distance from the confluence (km)	Latitude (°)	Longitude (°)	Gully drainage area (km^2)	Gully gradient	Fan gradient	Excess topography Z_E (m)	Frequency (yr^{-1})	Sediment size		
								5-1cm (%)	1-0.1cm (%)	0.1-0.01cm (%)
13.2	35.52924	100.005	0.5854	0.217	0.143	295	0.4	66	19	15
13.6	35.53133	100.0006	1.0908	0.205	0.165	267	0.4	59	22	19
13.6	*99.9943*	*35.519974*	*0.0300*	*0.400*	*0.067*	*12*		*13*	*22*	*65*
14.3	35.53188	99.99242	0.5884	0.110	0.143	289	1.7	58	23	19
14.6	35.533	99.98952	1.1417	0.162	0.155	269		57	24	18
14.9	*99.97925*	*35.525943*	*0.0400*	*0.380*	*0.057*			*14*	*23*	*63*
15.1	35.53402	99.98448	0.2706	0.270	0.192	268	0.5	57	26	18
15.3	35.53488	99.98188	0.3229	0.171	0.152	330	0.6	56	22	22
15.7	35.53398	99.97746	0.8247	0.198	0.153	265		53	23	24
16.1	35.5351	99.97299	0.5694	0.229	0.183	190	0.5	56	25	19
16.4	35.53457	99.96956	2.8022	0.098	0.165	213		62	24	14
17.3	35.53627	99.95997	0.3782	0.225	0.232	326		60	23	17
17.5	35.53719	99.9583	0.5865	0.214	0.143	293		65	23	12
18.4	35.54167	99.94968	0.6516	0.242	0.163	281	0.8	62	23	15
19	35.54684	99.94355	0.4577	0.292	0.142	330		66	23	11
19.4	35.54896	99.94055	0.3577	0.337	0.272	346	1.2	65	23	12
19.7	35.55072	99.93725	0.3640	0.292	0.272	350		63	23	14
20.1	35.55368	99.93431	0.2206	0.293	0.238	215		66	23	11
20.4	35.55567	99.93135	0.2564	0.277	0.248	252		62	23	15
20.8	35.55794	99.92759	1.4680	0.133	0.155	120		69	22	9
21.1	35.55998	99.92437	0.4849	0.189	0.152	320	1.5	62	22	16
21.4	35.56293	99.92209	0.4794	0.169	0.132	312		63	22	15
22.4	35.5709	99.91449	0.9976	0.129	0.193	140	0.9	61	22	17
22.9	35.57198	99.90871	0.3624	0.231	0.232	367		61	22	17
23.2	35.5728	99.90605	2.7850	0.092	0.135	223	0.2	61	22	18
23.6	35.57491	99.90235	0.2167	0.199	0.278	176	0.7	60	26	14
23.8	35.57529	99.89996	0.3168	0.249	0.272	320		60	23	18
24	35.57598	99.8979	0.5110	0.159	0.163	311		59	25	16
24.3	35.57752	99.89457	1.7100	0.116	0.145	253		59	26	16
24.8	35.57766	99.88819	0.0910	0.270	0.219	99				
25.2	35.57775	99.88489	2.0751	0.114	0.135	240	0.3	58	26	16
25.7	35.58099	99.87978	0.2877	0.223	0.278	250		58	22	21
25.9	35.57514	99.87266	0.0552	0.476	0.220	62				
26.2	35.58202	99.87495	0.1938	0.216	0.247	235		57	25	18
26.3	35.58276	99.87369	0.0589	0.310	0.162	59				
27.1	35.57586	99.86995	0.0606	0.449	0.405	65				
28.2	35.59525	99.85772	4.0584	0.072	0.125	150		57	26	18
29.1	35.57743	99.86794	0.0726	0.488	0.238	55				
30	35.58253	99.85927	0.0895	0.385	0.230	59				
30.1	35.58566	99.85678	0.1425	0.319	0.208	146				

Distance from the confluence (km)	Latitude (°)	Longitude (°)	Gully drainage area (km^2)	Gully gradient	Fan gradient	Excess topography Z_E (m)	Frequency (yr^{-1})	Sediment size		
								5-1cm (%)	1-0.1cm (%)	0.1-0.01cm (%)
30.2	35.58731	99.85302	0.0825	0.364	0.189	78				
30.3	35.59034	99.85062	0.1183	0.318	0.212	170				
30.3	*99.8371*	*35.605478*	*0.0450*	*0.390*	*0.068*	*11*		*15*	*19*	*66*
30.4	35.59167	99.84938	0.0691	0.343	0.245	255				
30.5	35.59412	99.84542	0.0617	0.326	0.333	89				
31.2	35.62013	99.83482	0.9600	0.188	0.143	280		56	25	19
31.3	35.61889	99.82783	1.1270	0.078	0.193	258				
31.8	35.62173	99.8238	0.1295	0.278	0.149	148				
31.9	35.62232	99.82169	0.0922	0.310	0.172	89				
35.6	35.64913	99.79838	5.2879	0.127	0.072	136	0.1	56	26	19
36	35.65078	99.79156	0.7443	0.129	0.198	283				
36.3	35.65287	99.79031	0.0739	0.309	0.219	59				
36.9	35.65784	99.78713	0.1724	0.244	0.211	265				
37.3	35.66069	99.78501	0.1646	0.261	0.211	130				
38.8	35.67564	99.77577	3.9959	0.148	0.175	176		55	26	19
39	35.66353	99.78839	4.6452	0.186	0.184	142				
40	35.67112	99.78078	0.3803	0.188	0.354	345				
40.3	35.69203	99.76765	6.2063	0.130	0.062	62		55	26	19
42.1	*99.76829*	*35.692476*	*8.0000*	*0.060*	*0.013*	*21*		*10*	*18*	*72*
42.5	35.71368	99.75625	5.6931	0.069	0.082	154	0.1	54	26	20
42.7	*99.69796*	*35.779035*	*0.0500*	*0.420*	*0.046*	*14*		*11*	*27*	*62*
42.9	35.72176	99.75734	4.8472	0.161	0.135	164		54	27	20
43.3	35.72685	99.75675	2.3308	0.167	0.145	223		53	27	20
44.8	35.74248	99.75008	1.4847	0.134	0.195	130	0.2	53	27	21
46.3	99.74747	35.75108	2.1455	0.124	0.135	230	0.5	52	27	21
46.5	99.74384	35.76143	3.5422	0.049	0.145	210	0.1	55	27	18
46.7	99.74022	35.77179	0.9344	0.130	0.153	274	1	60	28	12
46.9	99.73659	35.78215	1.1161	0.141	0.155	268	0.7	66	28	6
47.1	99.73296	35.79251	0.4797	0.220	0.192	302	1.8	65	28	7
47.2	99.72933	35.80286	0.6123	0.214	0.143	285	1.2	61	28	11
47.4	99.7257	35.81322	0.1469	0.327	0.297	143	0.5	65	26	9
47.6	99.72208	35.82358	0.2337	0.294	0.278	168	0.7	63	23	15
47.8	99.71845	35.83393	0.2480	0.266	0.238	253	0.6	62	25	13
47.8	99.71482	35.84429	0.1310	0.311	0.247	123	1	61	26	13
49.3	99.7112	35.85465	0.0764	0.350	0.257	55	0.4	60	24	16
50.8	99.70757	35.86501	0.2621	0.339	0.248	219	0.6	60	23	17
52.4	99.70394	35.87536	0.2807	0.383	0.258	243	0.7	59	23	18
53.9	99.70031	35.88572	0.0440	0.410	0.297	100	0.1	58	22	19
55.4	99.69669	35.89608	0.2103	0.382	0.248	150	0.3	58	22	21
56.7	*99.55672*	*35.802543*	*0.0600*	*0.390*	*0.037*	*16*		*12*	*16*	*72*

Distance from the confluence (km)	Latitude (°)	Longitude (°)	Gully drainage area (km^2)	Gully gradient	Fan gradient	Excess topography Z_E (m)	Frequency (yr^{-1})	Sediment size		
								5-1cm (%)	1-0.1cm (%)	0.1-0.01cm (%)
56.9	99.73633	35.76508	0.1541	0.413	0.267	124	0.7	57	21	22
58.4	99.72455	35.77262	0.4657	0.246	0.192	341	2	56	21	23
59.9	99.7075	35.78084	0.2809	0.446	0.278	233	0.7	56	20	25
61.4	99.70049	35.78277	0.2935	0.347	0.288	290	0.8	55	19	26
62.5	*99.50131*	*35.830368*	*6.0000*	*0.080*	*0.018*	*35*		*11*	*17*	*72*
62.9	99.69137	35.78751	0.3756	0.225	0.252	358	1.5	66	19	15
64.4	99.68301	35.79341	0.1649	0.363	0.297	130	0.9	62	18	20
65.9	99.66812	35.79791	0.3886	0.345	0.262	356	2	63	18	19
67.5	99.65088	35.80052	0.5621	0.228	0.153	295	2	65	23	12
67.6	*99.38037*	*35.922302*	*0.1000*	*0.340*	*0.044*	*42*		*10*	*18*	*72*
68.5	*99.27017*	*36.008379*	*0.0800*	*0.350*	*0.035*	*39*		*9*	*26*	*65*
69	99.62595	35.80523	0.2104	0.454	0.238	164	0.4	66	26	8
70	99.59568	35.80406	0.2970	0.415	0.228	300	0.8	60	25	15
72	*99.68962*	*35.7915*	*0.1200*	*0.211*	*0.016*	*0.1*			*14*	*86*
74	*99.67755*	*35.796151*	*0.5700*	*0.163*	*0.036*	*0.2*			*14*	*86*
76	*99.66271*	*35.796319*	*1.3200*	*0.191*	*0.041*	*0.1*			*16*	*84*
78	*99.65354*	*35.800109*	*4.6727*	*0.083*	*0.034*	*0.2*			*18*	*82*
80	*99.18229*	*35.887969*	*0.0562*	*0.241*	*0.042*	*0.5*			*12*	*88*
83	*99.64514*	*35.800088*	*0.1011*	*0.213*	*0.042*	*1*			*11*	*89*
83.6	*99.639*	*35.801443*	*0.1554*	*0.169*	*0.054*	*0.2*			*16*	*84*
84.2	*99.63168*	*35.801634*	*0.1249*	*0.294*	*0.064*	*0.3*			*17*	*83*
84.9	*99.62424*	*35.800366*	*4.3479*	*0.136*	*0.042*	*0.2*			*18*	*82*
86.1	*99.61434*	*35.796401*	*3.3651*	*0.185*	*0.042*	*0.1*			*12*	*88*
98	*99.20092*	*35.755107*	*3.6125*	*0.094*	*0.049*	*0.3*			*11*	*89*
128.6	*99.26199*	*35.767496*	*0.4746*	*0.200*	*0.046*	*0.1*			*14*	*86*
128.8	*99.26339*	*35.765941*	*0.3756*	*0.250*	*0.065*	*0.2*			*17*	*83*
129.5	*99.6074*	*35.79416*	*0.6251*	*0.247*	*0.045*	*0.1*			*14*	*86*
130.5	*99.59598*	*35.790432*	*0.3665*	*0.292*	*0.040*	*0.1*			*16*	*84*
131.4	*99.59109*	*35.788446*	*0.6524*	*0.154*	*0.039*	*0.2*			*13*	*87*
134.8	*99.58517*	*35.787432*	*5.3185*	*0.155*	*0.049*	*0.1*			*13*	*87*
135.3	*99.53571*	*35.819295*	*4.9753*	*0.126*	*0.047*	*0.01*			*12*	*88*
137.7	*99.50329*	*35.83401*	*4.4654*	*0.128*	*0.020*	*0.02*			*16*	*84*
138.4	*99.42398*	*35.874163*	*6.4232*	*0.093*	*0.032*	*0.02*			*13*	*87*
140.8	*99.36719*	*35.942274*	*7.3348*	*0.075*	*0.033*	*0.01*			*15*	*85*